

We are IntechOpen, the world's leading publisher of Open Access books Built by scientists, for scientists

6,900

Open access books available

186,000

International authors and editors

200M

Downloads

Our authors are among the

154

Countries delivered to

TOP 1%

most cited scientists

12.2%

Contributors from top 500 universities



WEB OF SCIENCE™

Selection of our books indexed in the Book Citation Index
in Web of Science™ Core Collection (BKCI)

Interested in publishing with us?
Contact book.department@intechopen.com

Numbers displayed above are based on latest data collected.
For more information visit www.intechopen.com



Research of Lightweight Structures for Sandwich Core Model

Jeongho Choi

Abstract

The objective of this chapter is to focus on finding mechanical properties for two models defined as core-filled model (Type 1) and core-spaced model (Type 2) created by direct metal laser sintering (DMLS). Applied material is aluminum alloy AlSi10Mg powder and each model is created as a vertical additive manufacturing with DMLS. After quasi-static compression, Type 1 showed 19% higher elastic modulus, 12% higher compressive yield strength, and 51.6% higher elongation than Type 2. By uniaxial compressive test, there found two issues that can be the reasons to make weaker models by 3D printing were found: melted metals by DMLS are not connected with each other precisely and a space in additive layer when additive manufacturing makes a shape of specimen. In addition, anisotropy is the significant factor to decide stiffness or strength. In nearby future, various kinds of unit models such as core-filled or core-spaced model hope to be made a sandwich core structure and to be investigating more deeply about bending or shear properties continuously. In the near future, it is hoped that we see more upgraded 3D printing techniques for making aerospace materials.

Keywords: cellular solids, open cell unit model, closed cell unit model, honeycomb, stiffness, strength

1. Introduction

Generally, solid is composed of stereoscopic structure. The stereoscopic structure is a model based on two-dimension, three-dimension, and four-dimension in a space. The two-dimension is two axis like horizontal direction and vertical direction in a plane. The three-dimensional structure has three axes such as x, y, and z coordination, for instance, a vector. The four-dimensional structure has four axes such as optical illusion, for example, a cubic box. If the box is torn at every corner, then it can make a two-dimensional plane. If it is folded up, it can make a cubic box. This is called as tesseract, hypercube, or 8-cell regular octachoron. These are based on a geometrical concept in mathematics. It is the four-dimensional object called as hypercube or tesseract shown in **Figure 1**.

Applications of the hypercube were shape or size optimization for non-probabilistic description of uncertainty as computer aided optimum design of structure [1], optimal communication algorithms for hypercubes [2], parallel computing on a hypercube [3], structure connectivity [4], and so on.

It is interested in to create a unit cell model like honeycomb or open-cell in a sandwich core structure.

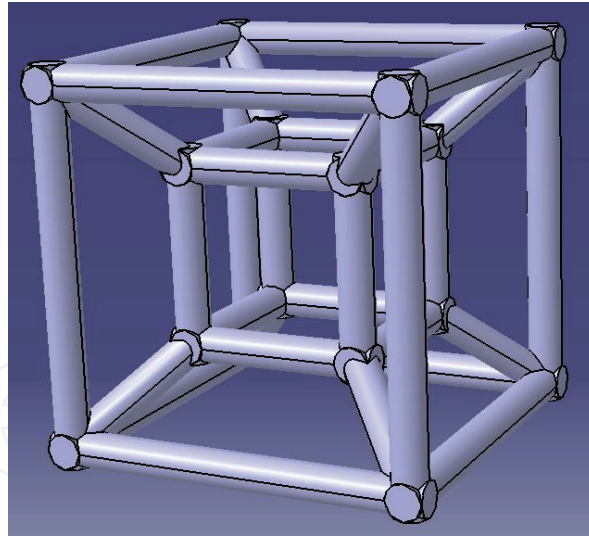


Figure 1.
Schematic of a hypercube.

Hypercube originates from a point, which is a hypercube of dimension zero [5, 6]. If the point moves to another point, it makes a line, which is a unit hypercube of dimension one. If the line moves out in a perpendicular direction, it makes a square, which is a unit hypercube of dimension two. If the square moves to a perpendicular direction, it makes a cube, which is a unit hypercube of dimension three. And if the cube moves to the fourth dimension, it is called a four-dimensional hypercube as a unit tesseract.

In the engineering material field, one of the simplest lightweight truss model is truss cubic, which is defined by Gibson and Ashby [7]; it is a model of hexagonal truss to define an ideal solution for honeycomb, open cell, or closed cell model. This is based on the three-dimensional stereoscopic structure. It can create a model which is hypercube truss model composed of a hexagonal truss inside and a hexagonal truss inside. Thus, this paper is focused on studying the hypercube concept to make a unit model to apply for a sandwich core structure.

If tesseract is composed of two regular hexahedrons, i.e., one is for outer structure and the other is for inner structure, with or without diagonal truss, then two types of model can be defined such as the core-filled or the core-spaced shape. That is, it depends with or without a truss in a diagonal direction. Therefore, this paper is focused on studying two models defined as Type 1 and Type 2.

According to the reported papers on the mechanical properties of structures that are 3D printed with powders recently, there are advantages and disadvantages.

The merits are to make a shape easily, to save time, to create a complex shape without any limited shape, and to make a high-quality part for the application in the aerospace or biomedical industry. Demerits are a high cost to create a product, a limited space to make a product, a limited materials such as metal powders, a required high quality equipment to produce high quality product, a need to hire a professional engineers to take control the equipment, etc.

Three-dimensional printing skill is not a magic to create anything; it requires techniques to be used with materials. The most important is what the application is. Thus, depending on the skills of the materials, the quality of a product is decided. Recently, 3D printing skill is announced as a revolution in manufacturing technique and it has been developed more and more. From the beginning of the skill, it is defined various techniques like fused deposition modeling (FDM) [8, 10], selective laser sintering (SLS) [9], direct light processing (DLP) [7, 8, 12], stereolithography (SLA) [11, 13], laminated object manufacturing (LOM) [11, 14], stereolithography (SL) [14], mask projection stereolithography (MPSL) [14], three-dimensional printing (3DP) [14], droplet

deposition manufacturing (DDM) [14], and fused filament fabrication (FFF) [15, 16]. Based on these techniques, new skills are currently being developed and announced.

Nowadays, a common skill of the 3D printing is direct metal laser sintering (DMLS) [17, 18]. It uses laser with metal powders, which is Laser beam melt metal powders to be droplet as liquid status. The drip metal is added layer by layer to make a shape.

To validate mechanical properties, tension and compression with a specimen made by ASTM standard are required. Many researchers found a specimen made by 3D printing have anisotropy and they shows mechanical properties are not shown in constant. They carried out experiments with different materials and with 3D printing. However, they show different properties depending on the 3D skill, equipment, applying material, additive manufacturing speeding, and so on. There are many kinds of effective variables [19–24].

This chapter concentrated on the investigation of stiffness or strength for unit cell models made by DMLS 3D printing. And it is hope to find mechanical properties of various unit models to make a sandwich core structure.

2. Hypercube models

For designed models, it is defined as an ideal mathematical solution. Based on the previous researchers, lattice or truss model defined as open cell model may have a correlation between relative elastic modulus as a function of relative density or between relative compressive yield strength as a function of relative density. Thus, **Figure 2** shows Type 1 and Type 2 shape. The next section shows details on stiffness or strength for both the models. Type 1 is core-filled model and Type 2 is a core-spaced model. Each model is created by the DMLS technique. And then both models are tested by compression. Before experimental testing for Type 1 and Type 2, they are checked for material properties of a specimen based on ASTM E8/E8M [25]. The specimen is made by DMLS and then tested by tension and compression to check the material properties.

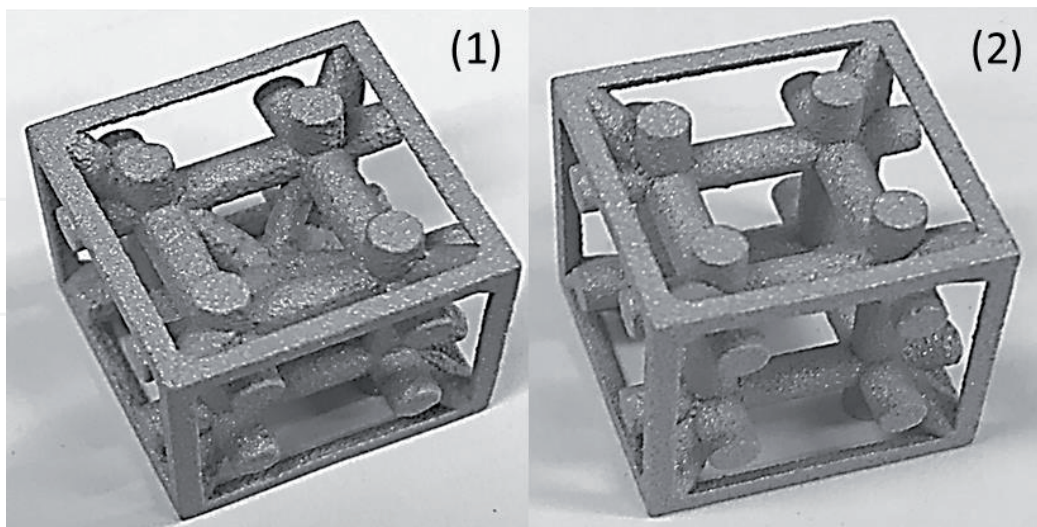


Figure 2.
Samples made by the 3D printing DMLS skill: (1) is Type 1 and (2) is Type 2.

3. 3D printing equipment (DMLS)

It used 3D printing machine which is defined as EOS M290. This is the DMLS (Direct Metal Laser Sintering) skill to make a specimen. It has a property summarized in **Table 1**. It shows more detailed information for the equipment. Among

Technical data EOS M290	
Building volume (mm)	250 × 250 × 325
Laser type (W)	Yb fiber laser; 40
Precision optics	F-theta lens; high-speed scanner
Scanning speed (m/s)	Up to 7.0
Focus diameter (μm)	100
Power supply (A/V)	32/400
Power consumption (kW)	Max. 8.5/average 2.4/with platform heating up to 3.2
Inert gas supply (hPa)	7000
Dimensions	W × D × H
System (mm)	2500 × 1300 × 2190
Recommended installation space (mm)	Min 4800 × 3600 × 2900
Weight(kg)	In approx. 1250
Software	EOSTATE Everywhere, EOSPRINT incl. EOS PArAmeterEditor
Materials	EOS Aluminum AlSi10Mg, EOS CobaltChrome MP1, EOS Maraging Steel MS1, EOS NickelAlloy HX, EOS NickelAlloy IN625, EOS NickelAlloy IN718, EOS StainlessSteel CX, EOS StainlessSteel PH1, EOS StainlessSteel 17-4PH, EOS StainlessSteel 316 L, EOS Titanium Ti64, EOS Titanium Ti64ELI, EOS Titanium TiCP Grade2
Optional accessories	EOSTATE Monitoring Suite (EOSTATE Laser, EOSTATE PowerBed, EOSTATE MeltPool, EOSTATE Exposure OT). Comfort Power Module, IPCM-M extra, IPCM-M pro, wet separator blasting cabinet

Table 1.
Technical data of DMLS equipment.

these, one of the most important factors is building volume and power supply for the laser. Maximum size of volume to make a model is 250 mm × 250 mm × 325 mm. To make a good quality model, volume size must be 200 mm × 200 mm × 300 mm at least. And laser type is Yb fiber laser with 40 Watt, scanning speed is up to 7.0 m/s, and power supply is 32 ampere with 400 Volt. In addition, more information for the equipment such as dimensions, weight, software, applying materials, etc., is described in the table, especially, materials that have been developing continuously. Now they can obtain materials like aluminum alloy, cobalt chrome, nickel alloy, stainless steel, and titanium alloy. These are based on powder type.

Technical data for aluminum alloy is shown in **Table 1** and 3D printing machine, EOS M290, based on DMLS skill.

4. Material properties (powder)

Applied material properties in this paper is aluminum alloy, which is AlSi10Mg. Based on ASTM E8M, specimens for compression and tension are made by the DMLS (direct metal laser sintering) 3D printing technique. **Figure 3** shows specimens after tensile test.

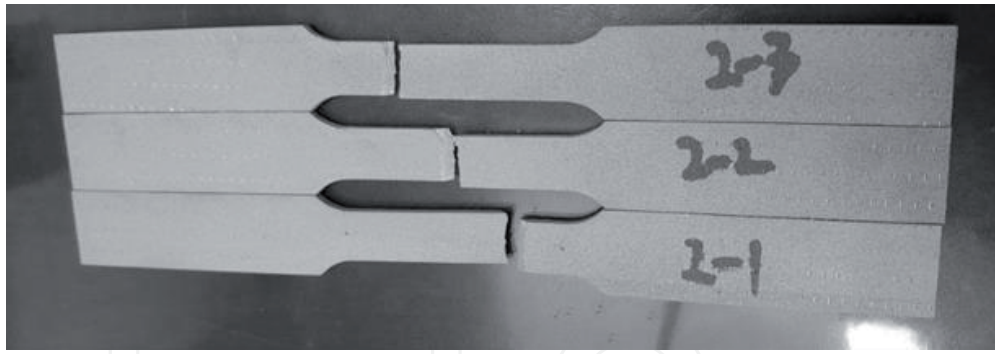


Figure 3.
 Specimens made by aluminum alloy (AlSi10Mg) after tension test.

Typical achievable part accuracy (μm)	± 100		
Smallest wall thickness (mm)	Approx. 0.3–0.4		
Surface roughness, as built, cleaned (μm)	Ra 6–10, Rz 30–40		
-after micro shot-peening (μm)	Ra 7–10, Rz 50–60		
Volume rate (mm^3/s)	7.4		
Physical and chemical properties of the parts			
Material composition (wt%)	Al (balance), Si (9.0–11.0), Fe(≤ 0.55), Cu(≤ 0.05), Mn(≤ 0.45), Mg(0.2–0.45), Ni(≤ 0.05), Zn(≤ 0.10), Pb(≤ 0.05), Sn(≤ 0.05), Ti(≤ 0.15)		
Relative density (%)	Approx. 99.85		
Density (g/cm^3)	2.67		
Mechanical properties of the parts			
		As built	Heat treated
Tensile strength (MPa)	In horizontal direction (XY)	460 \pm 20	345 \pm 10
	In vertical direction (Z)	460 \pm 20	350 \pm 10
Yield strength, Rp0.2%(MPa)	In horizontal direction (XY)	270 \pm 20	230 \pm 20
	In vertical direction (Z)	240 \pm 20	230 \pm 20
Modulus of elasticity (GPa)	In horizontal direction (XY)	75 \pm 10	70 \pm 10
	In vertical direction (Z)	70 \pm 10	60 \pm 10
Elongation at break (%)	In horizontal direction (XY)	9 \pm 2	12 \pm 2
	In vertical direction (Z)	6 \pm 2	11 \pm 2
Hardness (HBW)		Approx. 119 \pm 5	—
Fatigue strength (MPa)	In vertical direction (Z)	Approx. 97 \pm 7	—

Table 2.
 Technical data for aluminum alloy AlSi10Mg powder (wt = weight, approx. = approximately).

AlSi10Mg is a casting alloy and powder type. It can be used in the field for the combination of good thermal properties and low weight. **Table 2** contains technical data for AlSi10Mg powder. It shows general process, geometrical data, physical and chemical properties of the parts, mechanical properties of the parts, and thermal properties of parts.

5. Experimental setup

A mechanical type-universal test machine (UTM) is obtained for the tension or compression test. UTM is DTU-900MHA and a mechanical type with a digital signal processor (DSP) system as shown in **Figure 4**. For the tension test, **Figure 5** shows experimental setup in the UTM. It shows uniaxial tensile test with specimen made by aluminum ally, AlSi10Mg. **Figure 5(1)** is a specimen before tensile test and **Figure 5(2)** shows a specimen after the tensile test. **Figure 5(2)** shows a circle which means zoom-out as the right figure. The right figure shows a good tested result in the specimen, because it is broken in middle area in the specimen



Figure 4.
Universal test machine (UTM) with data collector system.

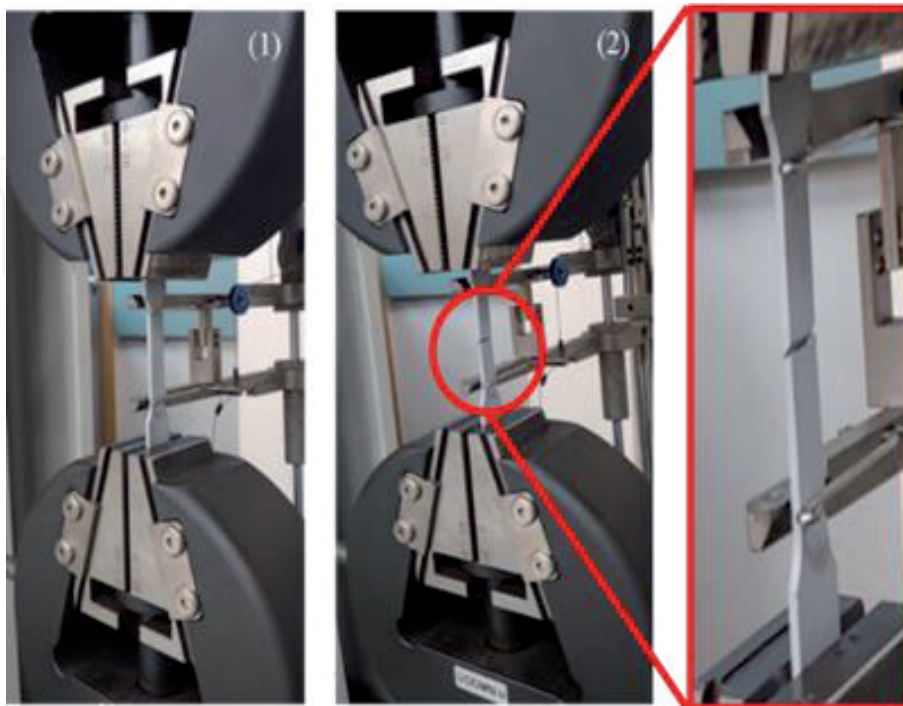


Figure 5.
Uniaxial tensile test with specimen made by aluminum alloy AlSi10Mg. Test speeding is set up as 1 mm/min: (1) shows a specimen before testing; (2) shows a specimen after testing.

as setup with mechanical extensometer. Test speeding in the UTM is setup as 1 mm per a minute.

6. Tension

Making a tensile specimen is based on ASTM E8M standard. The specimens were obtained by AlSi10Mg power with the DMSL technique. Each section defined as a letter which shows dimensions on **Table 3**. **Table 3** shows rectangular shape of tension test specimens with detail dimensions like the gauge length, width, thickness, radius of fillet, overall length, length of reduced section, a length of grip section, and an approximate width of grip section. Thus, DMLS made specimens for the tension test.

Totally, three samples made by aluminum alloy (AlSi10Mg) marked as 2-1, 2-2, 2-3 were ready for the tension test, and they were tested by uniaxial tensile testing.

Figure 6 shows specimens after tensile test and results with (a) engineering stress-engineering strain for all specimens and (b) stress-strain for 2-2 specimen. As you can see, 2-2 specimen shows clearly that the middle point was broken. Others were broken in an area of top point or bottom point. Thus, tested data were selected for 2-2 specimen because it shows a good fracture.

From the tension test, engineering stress-strain and true stress-strain can be defined as shown in **Figure 6**. **Figure 6** shows a comparison between engineering stress-strain and true stress-strain for aluminum alloy AlSi10Mg.

Dimensions of standard specimens, sheet-type [mm]	
Gauge length	50.0 ± 0.10
Thickness	3.0
Radius of fillet, min	12.5
Overall length, min	200
Length of reduced section, min	57
Length of grip section, min	50
Width of grip section, approximate	20

Table 3.
 Rectangular tension test specimens based on ASTM E8M.

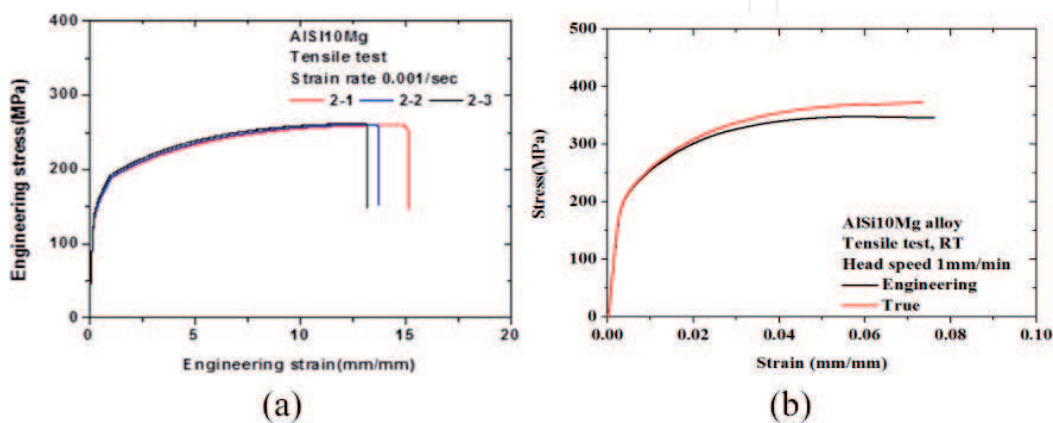


Figure 6.
 Stress as a function of Strain for Aluminum alloy specimen after tensile test; (a) Engineering stress - Engineering strain for all specimens, and (b) Stress-strain for 2-2 specimen.

Material	Properties	Value
AlSi10Mg	Young's modulus (GPa)	71.8
	Yield strength (MPa)	155.5
	Ultimate tensile strength (MPa)	348.3
	Elongation (%)	8.0

Table 4.
Mechanical properties of AlSi10Mg by tension.

In order to do the tension test for AlSi10Mg, its defined material properties are as follows: Young's modulus is 71.81 GPa, yield strength is 155.52 MPa, and ultimate tensile strength is 348.32 MPa approximately. These are summarized in **Table 4**. When the Young's modulus value is compared in **Table 2**, they almost matched in vertical direction. That is, it is proved that tensile specimen is created in vertical direction by DMLS.

7. Compression

Specimens for uniaxial compression test are made by the 3D printing DMLS technique as shown in **Figure 7**. It was made by the same equipment as EOS M290 and the same material as aluminum alloy, AlSi10Mg. The sample size is designed as diameter is 10 mm and height is 15 mm as shown in **Figure 7**. The figure also shows real specimens made by aluminum alloy. For the compression test, three specimens are ready.

Two specimens are used for the compression test because both samples are almost matched in the stress-strain plot shown in **Figure 8**. Thus, material properties for the compression test with Al alloy, AlSi10Mg, are defined as follows: Young's modulus is 0.316 GPa, yield compressive yield strength is 6.35 MPa, and ultimate compressive strength is 179.72 MPa. **Figure 8** shows the crushing 6 steps within a range of 0–0.6, strains and each step is defined as: ① is elastic range,

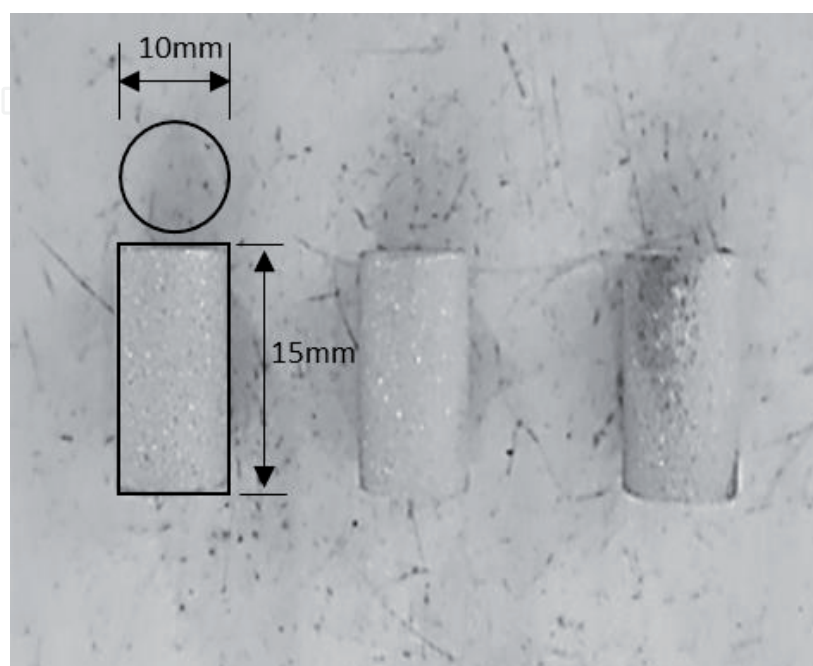


Figure 7.
Designation and AlSi10Mg specimens for compression test.

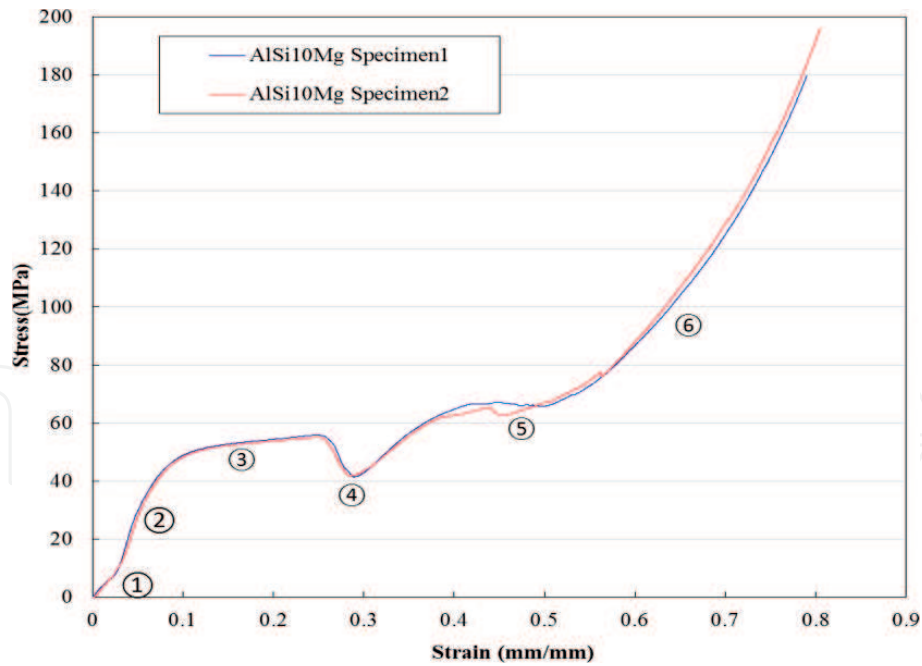


Figure 8.
 Crushing steps such as ① elastic range, ② linear, ③ 1st plateau, ④ valley, ⑤ 2nd plateau, and ⑥ densification.

② linear, ③ the 1st plateau, ④ valley, ⑤ the 2nd plateau, and ⑥ densification. Thus, Young’s modulus is checked in elastic range ①. Linear ② shows increasing loads. Then, 1st plateau shows in ③. In here, loading slowly increase. Valley ④ shows as being abruptly dropped, because belly phenomenon happened in the middle of 15 mm height specimen. It means endurance of applied loading in specimen is over. Then, it shows the 2nd plateau as ⑤ where applied loads slowly decreased. This means applied stress is distributed in specimen. At the end, densification ⑥ is shown.

8. 4D cube mechanical test

There are two types of model for mechanical testing. The two models are core-spaced model defined as Type 1 and core-filled model defined as Type 2. **Figure 2** shows two samples that are made by the 3D printing DMLS skill. Each sample is

Applied material	Sample type	Sample number	Width (mm)	Length (mm)	Height (mm)	Truss diameter (mm)		Weight (grams)
						Outer	Inner	
AlSi10Mg	Type 1	1	20	20	20	1.5	3	5.91
		2	20	20	20	1.5	3	5.91
		Average	20	20	20	1.5	3	5.91
	Type 2	1	20	20	20	1.5	3	5.29
		2	20	20	20	1.5	3	5.29
		Average	20	20	20	1.5	3	5.29
Difference								11.72%

Table 5.
 Measured weights for Type 1 and Type 2 model made by AlSi10Mg alloy.

designed as width 20 mm, length 20 mm, height 20 mm, inner truss diameter 3 mm, and outer truss radius 1.5 mm. Type 1 is core-spaced model shown in **Figure 2(1)** and Type 2 is core-filled model shown in **Figure 2(2)**.

Before the uniaxial compression test, measured weight for Type 1 is 5.91 grams and Type 2 is 5.29 grams. Difference between Type 1 and Type 2 is about 11.72% in weights. Details are summarized in **Table 5**.

Applied material is Al alloy and powder type shown in **Table 2**. Applied speed in the UTM machine is defined as 2 mm per minute. Type 1 is core-filled model

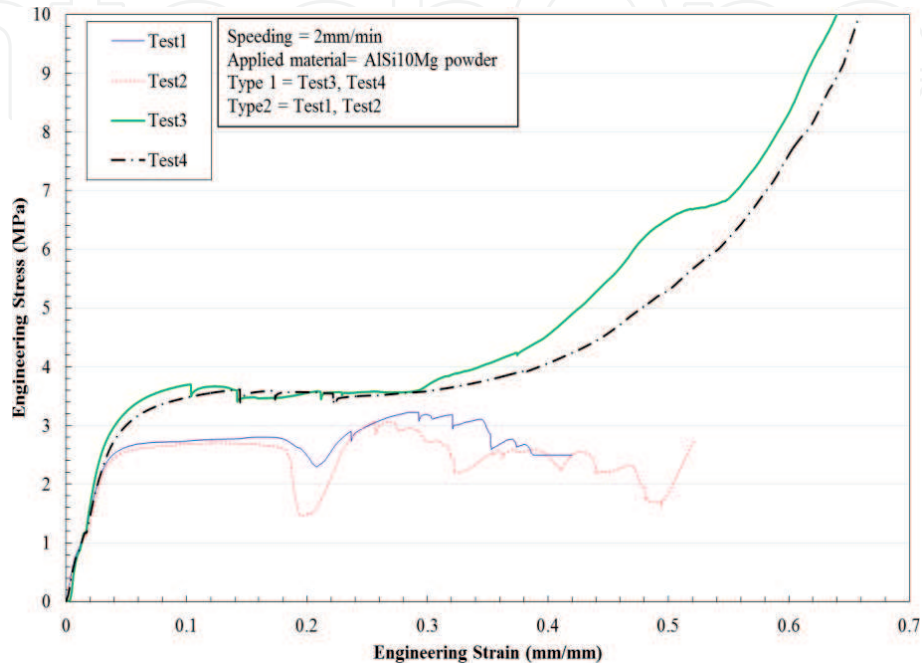


Figure 9. Engineering stress as a function of engineering strain from uniaxial compression.

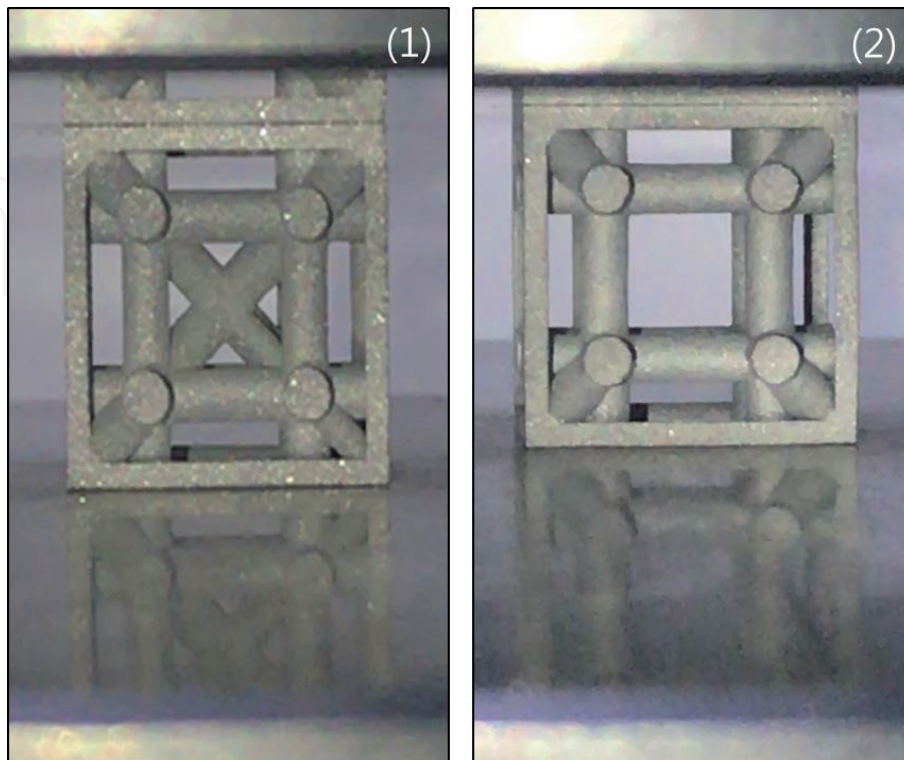


Figure 10. Uniaxial compression test in UTM for (1) Type 1 and (2) Type 2.

Type	Sample number	Material properties			
		Young's modulus (GPa)	Compressive yield strength (MPa)	Ultimate compressive strength (MPa)	Compressibility (%)
1	Test 3	0.92	2.60	13.40	70
	Test 4	0.72	2.54	11.47	68
	Average	0.82	2.57	12.44	69
2	Test 1	0.71	2.29	3.22	42
	Test 2	0.66	2.29	3.08	49
	Average	0.69	2.29	3.15	46
Difference		19.7%	12.2%	294.8%	51.6%

Table 6.
 Material properties of Type 1, core-filled model, and Type 2, core-spaced model.

of test 3 and test 4. Type 2 is core-spaced model of test 1 and test 2. Thus, tested result shows engineering stress as a function of engineering strain in **Figure 9**. Based on the compression test, **Figure 9** shows material properties for elastic modulus, compressive yield strength, ultimate compressive strength, compressibility, and so on. **Figure 10** shows setup for uni-axial compression test in UTM for (1) Type 1 and (2) Type 2 model.

For Type 1, the average values of material properties are elastic modulus is 0.82GPa, compressive yield strength is 2.57 MPa, ultimate compressive strength is 12.44 MPa, and percent compressibility is 69%, approximately. For Type 2, the average values of material properties are elastic modulus is 0.69GPa, compressive yield strength is 2.29 MPa, ultimate compressive strength is 3.15 MPa, and compressibility is 46%, approximately. **Table 5** summarizes the material properties of core-filled or core-spaced model. It shows differences between Type 1 for core-filled model and Type 2 for core-spaced model about material properties. For Young's modulus, core-filled model is higher 19.7%, compressive yield strength 12.2%, ultimate compressive strength 294.8%, and compressibility 51.6% than core-spaced model as summarized in **Table 6**.

9. Results

Material properties between core-filled model and core-spaced model are investigated. All models are based on aluminum alloy AlSi10Mg and they are made by the 3D printing DMLS technique. Finally, 4D cube models defined as core-filled as Type 1 and core-spaced as Type 2 are tested by compression. Thus, Type 1 shows a higher Young's modulus, compressive yield strength, compressive ultimate compressive strength, and compressibility. The reason is that Type 1 can endure outer loads with a diagonal truss connected with inside hexagonal truss structure. However, Type 2 can be broken easily because they do not have a diagonal truss supporting. It is simply connected with outer or inner hexagonal structure without a cross truss. Thus, Type 1 shows a general shape of compressive tested line on **Figure 9**.

However, Type 2 shows an elastic line, yield, plateau, and up down line in **Figure 9** as in test 3 and test 4. Here, the interest is in the up down line. When it is tracked by broken specimens, it is identified as a reason; that is, when specimens are made by the 3D printing DMLS skill, laser melt metal powder at first and then the

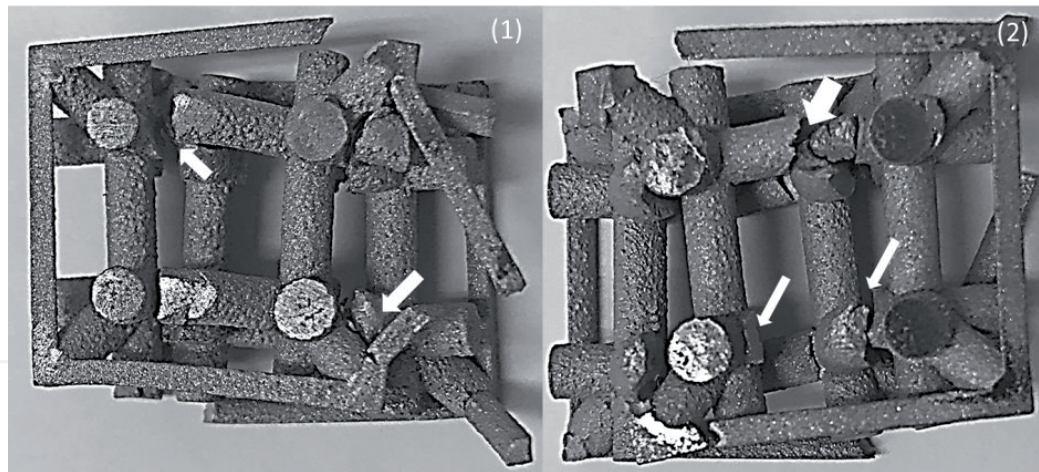


Figure 11.
Crushed samples shown as arrows: (1) core-filled model. (2) core-spaced model.

melted metal is added on each side of the truss clot by clot. Thus, each clot does not create perfect solid shape and it is not precisely connected with each truss. These are shown in **Figure 9**. Therefore, due to these reasons, material properties for 4D cube models made by the 3D printing DMLS skill show lower than solid material properties. Based on broken section in the sample (1) or (2) shown in **Figure 11**, there shows two issues. One is that melted metals are not connected with each other like a solid precisely. Due to this reason, connected sections in each model as Type 1 or Type 2 are easily broken after outer loading. These are shown as arrows in **Figure 11(1)** and (2). The other one is there shows a space in additive layer when additive manufacturing makes a shape of specimen. Because of the space in the additive layer, each truss created by melted metals does not have enough to support outer loadings.

10. Conclusion

This chapter focused on finding material properties for two models defined as core-filled model, Type 1, and core-spaced model, Type 2, created by the 3D printing direct metal laser sintering (DMLS) technique. The models use aluminum alloy AlSi10Mg powder with a skill of direct laser sintering. After the uniaxial compressive test, it is proved that core-filled model has an elastic modulus of 19.7%, compressive yield strength of 12.2%, ultimate strength of 294.8%, and percentage of elongation of 11% higher than core-spaced model. It also shows core-filled model have a higher strength but core-spaced model shows a lower strength after compression. There shows two issues that melted metals by DMLS skill are not connected with each other like a solid precisely and there shows a space in additive layer when additive manufacturing makes a shape of specimen. These issues are the main reasons for weaker strength or lower elastic modulus in the models. It is hoped that the two models be made sandwich core structure and then the structure be investigated more deeply. In nearby future, it is hope that 3D printing techniques such as FDM [8, 10], SLS [9], DLP [7, 8], SLA [11, 13], LOM [11, 14], SL [14], MPSL [14], 3DP [14], FFF [15, 16], or DMLS [17, 18] are applied into making hypercube models and then it is to do the testing to check what is the differences of mechanical properties are. In addition, it is expected that hypercube models are applied into make a sandwich panel and then they are to be obtained to find mechanical properties. Finally, it is hope that the sandwich panels will be approved to be selected as one of aerospace materials.

Acknowledgements

This research was supported by Basic Science Research Program through the National Research Foundation of Korea (NRF) funded by the Ministry of Education (grant number NRF-2018R1D1A1B07041383).

Conflict of interest

I confirm there are no conflicts of interest.

Notes/thanks/other declarations

Many thanks go to Dr. Sang-ik Lee for doing this project.

Author details

Jeongho Choi
School of Mechanical Engineering, College of Engineering, Kyungnam University,
Chang-won, Republic of Korea

*Address all correspondence to: choicaf@gmail.com

IntechOpen

© 2019 The Author(s). Licensee IntechOpen. This chapter is distributed under the terms of the Creative Commons Attribution License (<http://creativecommons.org/licenses/by/3.0>), which permits unrestricted use, distribution, and reproduction in any medium, provided the original work is properly cited. 

References

- [1] Eugenio B, Carlo C, Marco L. Shape/size of truss structures using optimization for non-probabilistic description of uncertainty. *Transactions on the Built Environment—Computer Aided Optimum Design of Structures V*. 1997;**28**:163-172. DOI: 10.2495/OP970161
- [2] Bertsekas DP, Ozveren C, Stamoulis GD, Tseng P, Tsitsiklis JN. Optimal communication algorithms for Hypercubes. *Journal of Parallel and Distributed Computing*. 1991;**11**:263-275. DOI: 10.1016/0743-7315(91)90033-6
- [3] Ostrouchov G. Parallel computing on a hypercube-An overview of the architecture and some applications. Oak Ridge National Lab. CONF-8703131-1. DOE: AC05-84OR21400
- [4] Mane SA. Structure connectivity of hypercubes. *AKCE International Journal of Graphs and Combinatorics*. 2018;**15**:1. DOI: 10.1016/j.akce.2018.01.009
- [5] Harary F. A survey of the theory of hypercube graphs. *Computers & Mathematics with Applications*. 1988;**15**:277-289. DOI: 10.1016/0898-1221(88)90213-1
- [6] Mane SA. Structure connectivity of hypercubes. *AKCE Int. J. Graphs Comb*. 2018;**15**:49-52. DOI: 10.1016/j.akcej.2018.01.009
- [7] Gibson LJ, Ashby MF. *Cellular Solids—Structure and Properties*. 2nd ed. Cambridge, United Kingdom: Cambridge University Press; 1997. DOI: 10.1017/CBO9781139878326
- [8] Song Y, Li Y, Song W, Yee K, Lee K-Y, Tagarielli VL. Measurements of the mechanical response of unidirectional 3D-printed PLA. *Materials & Design*. 2017;**123**:154-164. DOI: 10.1016/j.matdes.2017.03.051
- [9] Gibson I, Shi D. Material properties and fabrication parameters in selective laser sintering process. *Rapid Prototyping Journal*. 1997;**3**:129-136. DOI: 10.1108/13552549710191836
- [10] Kulkarni P, Dutta D. Deposition strategies and resulting part stiffnesses in fused deposition modeling. *Journal of Manufacturing Science and Engineering*. 1999;**121**:93-103. DOI: 10.1115/1.2830582
- [11] Feng P, Meng X, Chen JF, Ye L. Mechanical properties of structures 3D printed with cementitious powders. *Construction and Building Materials*. 2015;**93**:486-497. DOI: 10.1016/j.conbuildmat.2015.05.132
- [12] Hornbeck LJ. Digital light processing update: Status and future applications. In: *Proceeding SPIE3634, International Society for Optics and Photonics Projection Displays V (Electronic Imaging'99)*; 20 May 1999; San Jose, CA, United States. 1999. pp. 158-170
- [13] Ikuta K, Hirowatari K, Ogata T. Three dimensional micro integrated fluid systems (MIFS) fabricated by stereolithography. *Micro electro mechanical systems*. In: *Proceedings IEEE Micro Electro Mechanical Systems an Investigation of Mirco Structures, Sensors, Actuators, Machines and Robotic Systems (MEMS'94)*; 25-28 January 1994. Siso, Japan: IEEE Workshop on; IEEE; 1994. pp. 1-6
- [14] Engkvist G. Investigation of microstructure and mechanical properties of 3D printed Nylon [thesis]. *Materials Engineering: Lulea University of Technology*; 2017
- [15] Basgul C, Yu T, MacDonald DW, Siskey R, Marcolongo M, Kurtz SM. Structure-property relationships for 3D-printed PEEK intervertebral

lumbar cages produced using fused filament fabrication. *Journal of Materials Research*. 2018;**33**:2040-2051. DOI: 10.1557/jmr.2018.178

[16] Mohseni M, Hutmacher DW, Castro NJ. Independent evaluation of medical-grade bioresorbable filaments for fused deposition modelling/ fused filament fabrication of tissue engineered constructs. *Polymers*. 2018;**10**:1-17. DOI: 10.3390/polym10010040

[17] Kundu S, Hussain M, Kumar V, Mumar S, Das AK. Direct metal laser sintering of TiN reinforced Ti6Al4V alloy based metal matrix composite-fabrication and characterization. *The International Journal of Advanced Manufacturing Technology*. 2018;**97**:2635-2646. DOI: 10.1007/s00170-018-2159-7

[18] Alsalla HH, Smith C, Hao L. The effect of different build orientations on the consolidation, tensile and fracture toughness properties of direct metal laser sintering Ti-6Al-4V. *Rapid Prototyping Journal*. 2018;**24**:276-284. DOI: 10.1108/RPJ-04-2016-0067

[19] Cantrell J, Rohde S, D'Amiani D, Gurnani R, diSandro L, Anton J, et al. Experimental characterization of the mechanical properties of 3D printed ABS and polycarbonate parts. In: Yoshida S, Lamberti L, Sciammarella C, editors. *Advancement of Optical Methods in Experimental Mechanics*. In: *Proceedings of the Society for Experimental Mechanics Series Book Series (CPSEMS'17)*. Cham: Springer; 2017. pp. 89-105

[20] Leite M, Fernandes J, Deus AM, Reis L. Study of the influence of 3D printing parameters on the mechanical properties of PLA. In: *3rd International Conference on Progress in Additive Manufacturing (pro-AM 2018)*; 14-17 May 2018; Singapore. 2018

[21] Salet TAM, Ahmed ZY, Bos FP, Laagland HLM. Design of a 3D printed

concrete bridge by testing. *Virtual and Physical Prototyping*. 2018;**13**:222-236. DOI: 10.1080/17452759.2018.1476064

[22] Mehta LS, Pillai P. Compression testing of PLA in 3D printing. *International Journal of Electronics, Electrical and Computational System (IJEECS)*. 2017;**6**:466-470. ISSN: 2348-117X, DOI: No Data

[23] Divyathej MV, Varun M, Rajeev P. Analysis of mechanical behavior of 3D printed ABS parts by experiments. *International Journal of Scientific and Engineering Research*. 2016;**7**:116-124. ISSN: 2229-5518, DOI: No Data

[24] Hernandez R, Slaughter D, Whaley D, Tate J, Asiabanpour D. Analyzing the tensile, compressive, and flexural properties of 3D printed ABS P430 plastic based on printing orientation using fused deposition modeling. In: *Proceedings of the 27th Annual International Solid Freeform Fabrication Symposium—An Additive Manufacturing Conference Reviewed Paper (Solid Freeform Fabrication 2016)*. 2016. pp. 939-950

[25] ASTM E8/E8M-13. *Standard Test Methods for Tension Testing of Metallic Materials*. West Conshohocken, PA: ASTM International; 2013. Available from: www.astm.org. DOI: 10.1520/E0008_E0008M-13